Journal of Materials Research and Technology

Seeing the Big Picture: Improving The Prosthetic Design Cycle Using 360° 3D Digital Image Correlation
--Manuscript Draft--

Abstract:	Additive manufacturing is one of the most promising emerging technologies for building prosthetic sockets. However, there is no reliable way to estimate the factor of safety and the lifetime of 3D printed prosthetic sockets. Here, we explore 360° 3D digital image correlation (DIC) and discover how this new tool can increase our understanding of prosthetic structural failures. We establish that this new technology can dramatically improve the prosthetic design cycle by identifying local strain concentrations and by highlighting limitations in current simulated models. Overall, 360° 3D DIC technology empowers prosthetic engineers to characterize the performance of new materials and create innovative designs that are both safe and affordable.

Suggested Reviewers:	

	████████████████
Opposed Reviewers:	

Seeing the Big Picture: Improving The Prosthetic Design Cycle Using 360° 3D Digital Image Correlation

Isaac A. Cabrera[a,*], Joseph C. Martin[a], Samantha T. Fong[a], Kha H. M. Nguyen[b], Victor D. Bourgin[c], Win-Ying Zhao[a], KiAsia J. Lawson[d], Kaela A. Wong[a], Pegah Bagheri[a], Parker J. Hill[b], Bryn M. Henning[a], Patricia M. Castillo[b], Ramesh R. Rao[e], Marc A. Meyers[a,f], Albert Y. Lin[e], Joanna M. McKittrick[a]

a) Department of Mechanical and Aerospace Engineering, University of California San Diego, La Jolla, CA 92093-0411, United States
b) Department of Bioengineering, University of California San Diego, La Jolla, CA 92093-0411, United States
c) Department of Bioengineering, Imperial College London, South Kensington Campus, London, SW7 2AZ, United Kingdom
d) Department of Bioengineering, North Carolina Agricultural and Technical State University, Greensboro, NC 27411, United States
e) California Institute for Telecommunications and Information Technology (Calit2), La Jolla, CA 92093, United States
f) Department of Nanoengineering, University of California San Diego, La Jolla, CA 92093-0411, United States

*Corresponding Author: iacabrer@ucsd.edu
Present address: 3869 Miramar Street, Box 1236, La Jolla, CA 92037, United States

Abstract:

Additive manufacturing is one of the most promising emerging technologies for building prosthetic sockets. However, there is no reliable way to estimate the factor of safety and the lifetime of 3D printed prosthetic sockets. Here, we explore 360° 3D digital image correlation (DIC) and discover how this new tool can increase our understanding of prosthetic structural failures. We establish that this new technology can dramatically improve the prosthetic design cycle by identifying local strain concentrations and by highlighting limitations in current simulated models. Overall, 360° 3D DIC technology empowers prosthetic engineers to characterize the performance of new materials and create innovative designs that are both safe and affordable.

Keywords: Digital Image Correlation, Prosthetics, Structural Analysis, Failure

1. Introduction

Every year in the United States, more than 185,000 people lose their limbs to trauma, infection, malignancy, diabetes or other conditions and this number is projected to keep growing [1]. Around the globe, approximately 40 million individuals are amputees and as many as 95% of them do not wear a prosthetic [2]. Amputees who do not wear a prosthetic suffer from limited mobility as well as limited access to education, employment, and financial support [3]. 3D printing has been identified as a breakthrough technology that can dramatically improve access to affordable prosthetic limbs [4]. It can be used to manufacture customized prosthetics faster and more affordably than traditional shaping methods (**Figure 1**). Unfortunately, 3D printed prosthetic sockets are not currently safe enough to use in clinical practice. No polymeric 3D printed prosthetic socket to date has been sufficiently strong to comply with the loads specified by ISO 10328, the standard for structural testing of lower limb prosthetics [5]. For this reason, engineers need to understand how and why 3D printed sockets fail in order to improve their designs to the point where they can be utilized safely by amputees.

2. Background

2.1 Structural Analysis of Lower Limb Prosthetics

Prosthetic sockets are a critical structural component in lower limb prosthetics; however, they have not been tested or simulated to the same extent as other prosthetic components. This stems from the fact that prosthetic sockets are omitted from ISO 10328. These prosthetic sockets do not have the degree of mechanical analysis that load bearing structures should have. However, previous research on the topic yielded valuable insights into how to conduct experiments and analyze the failure of these prosthetic sockets. This previous work is framed in terms of the typical engineering design cycle: Simulation → Experiment → Simulation.

2.1.1 Prior Simulations

There are a significant number of simulations that seek to model the mechanical behavior of prosthetic sockets. Modeling prosthetic sockets is a challenge because it is a complex multi-body problem that involves interactions between multiple surfaces and materials with both linear elastic and viscoelastic behavior [6]. This has led to many different approaches for solving this complex simulation challenge dependent on some critical biomechanical assumptions. These simulations generally model this system to understand how a residual limb deforms in response to loading [6]. This perspective is limited because it does not evaluate the prosthetic sockets themselves for failure. However, the simulation parameters and boundary conditions can be modified to take this a step further for socket failure analysis.

Simulations of prosthetic sockets begin with obtaining a sample geometry. The most common approach utilizes magnetic resonance imaging (MRI) scans to obtain the hard and soft tissue geometry of a residual limb for simulations [7-10]. Material properties in these simulations are commonly simplified to homogeneous isotropic linear elastic behavior. More

sophisticated models utilize hyperelastic or viscoelastic formulations of material behavior [6, 7]. Loading and boundary conditions vary considerably based on the phase of the gait cycle. Most simulations utilize a pre-stress at a magnitude of 50 N. Standing yields static and vertical loading conditions while running or walking require ground reaction forces and moments [13, 14]. Simulations of donning, the act of putting on a socket, do not require pre-stresses [15]. The magnitude of stresses simulated was most commonly 800 N which is approximately 110% of an ideal patient's body weight [14-16]. In almost all cases of multibody simulations, the interface between the limb and socket was represented by a coefficient of friction (typically of value 0.5) [6, 7].

2.1.2 Prior Experiments

Failure in prosthetic sockets can be catastrophic. Amputees rely on sockets to maintain the link between their body and the prosthesis and they can be seriously injured in the event of failure. Therefore, engineers need to be able to verify and quantify the level of safety in prosthetic sockets. Simulations are useful tools for predicting these catastrophic events. However, because so many assumptions are made, experimental data is needed to validate these models. Despite the fact that ISO 10328 omits protocols for testing prosthetic sockets, several research teams have attempted to develop valid methods for testing the strength of these sockets. These tests are all inspired by ISO 10328 to specify the loading conditions for yield stress, ultimate strength, and fatigue strength of these sockets.

Current et al. [17] characterized the failure modes of composite prosthetic sockets in 1999. They developed a custom socket loading fixture (SLF) which enabled them to apply loads to a prosthetic socket with a 100kN hydraulic load cell. They identified three primary failure modes for the prosthetic socket material: inter-laminate shear, buckling, and tension. Significantly, they also noted that the prosthetic sockets failed near the pyramidal adapter. Most importantly, they noted that "none of the composite sockets in the study were able to meet the specified parameters set [by ISO 10328] for other prosthetic componentry."

Goh et al. [18] tested the mechanical strength of additively manufactured prosthetic sockets in 2002. They characterized the material properties of polypropylene sockets using ASTM D638 [19] and then tested for the strength of the prosthetic socket using ISO 10328 as a guideline. Both the static and cyclic (250,000 cycles) behavior was tested on prosthetic sockets in two loading configurations (standing and walking). The additively manufactured sockets failed catastrophically after the material reached its ultimate tensile strength.

Gerschutz et al. [20] performed an extensive strength evaluation of prosthetic sockets in 2012 (which is still the most comprehensive analysis to date). They developed a custom apparatus to test the static compressive strength of prosthetic sockets using an instrumented load cell and a standardized limb shape. Following this, they tested sockets manufactured by different providers around the United States. Their experiments revealed that check sockets (prototype sockets typically used for fitting) and copolymer sockets failed to meet the loading conditions specified by ISO 10328. This is significant because prosthetic sockets fabricated with 3D printing are very similar in strength to these check sockets.

Skoglund [21] built a custom apparatus to test the mechanical strength of prosthetic sockets manufactured by selective laser sintering (SLS) in 2015. This new apparatus represents

a significant improvement; it can apply compressive loads in a more biomechanically accurate manner by utilizing multiple ball joints. This new design also enables prosthetic sockets to be tested without geometrical modification. Using this new apparatus, Skoglund [21] was able to design a titanium alloy prosthetic socket to satisfy the ISO 10328 loading conditions.

2.2 Strain Characterization Advances

To understand how prosthetic sockets deform and fail, the most important tools for characterizing failure are experimental strain techniques. Strain gauges have been the primary method of characterizing mechanical performance of prosthetic sockets. However, new techniques for strain characterization have the potential to significantly improve the quality and quantity of experimental data.

2.2.1 Strain Gauges

Strain gauges have historically been the most frequently utilized tools for characterizing strain in prosthetics. Strain gauges work by outputting a voltage reading which changes over the course of an experiment; this voltage reading will decrease when a strain gauge undergoes extension because the resistance of the strain gauge increases. This technique has many advantages. Most importantly, it is relatively inexpensive and quantitative strain performance is very well documented. Strain gauges can be used on arbitrarily large structures as well as built into arrays to give information on the local strain field. Finally, strain gauges can be used in hollow structures to obtain interior strain information [22]. Disadvantages of strain gauges are that they fundamentally only give local uniaxial strain information, require perfect bonding for measurements, and can be complex to set up for large installations. These limitations have frustrated prosthetic researchers in the past who noted significant challenges in obtaining useful strain data [23].

2.2.2 Photoelasticity

The photoelasticity technique is equally well established for strain characterization being utilized as far back as 1932 [24]. In photoelasticity, light waves pass through a material that exhibits birefringence behavior under stress. The indices of refraction change in the material based on the induced polarization and which shifts the wavelength of light passing through a material and creates different colors which are used to determine stress and strain. The main advantage of this technique is that it can visualize stress and strain over an entire surface (including 3D surfaces), which yields significantly more information about a structure as a whole [25]. However, the photoelastic technique has its own limitations. It requires a part be made of a birefringent material. Otherwise, a relatively thick (~3 mm) uniform photoelastic coating must be adhered to the surface, possibly leading to reinforcement issues. Additionally, it can be tedious to calculate values of principal stress since it requires expensive equipment that is time consuming for 3D work [25, 26]. These factors have made photoelasticity unsuitable for use in prosthetic research.

2.2.3 Digital Image Correlation

Digital image correlation (DIC) is a relatively new technique for strain characterization, dating back to 1985 [27]. DIC works by tracking the displacement of an image pixel block on the surface of a sample. Simply by tracking these pixels, a computer can construct deformation vector fields and strain maps in both 2D and 3D. DIC only requires that the samples surface exhibit a unique pattern that can be easily tracked [28]. One main advantage of DIC is that the numerical strain is calculated automatically during the analysis, saving a great deal of time compared to photoelasticity. DIC has the additional advantage of not requiring a specialized coating. Some disadvantages of the technique are that it has primarily been restricted to 2D analysis because most implemented DIC algorithms assume plane strain and stress conditions [29]. 3D analysis has been dramatically improving in recent years, but the majority of analyses utilize small surfaces generated from a single stereo camera pair [30, 31]. 360° DIC systems have been developed commercially such as by Dantec Dynamics; however these solutions are extremely expensive. Two recent papers by Solav et al. [32, 33] outlined a new method called MultiDIC to stitch together an arbitrary number of stereo camera pairs. This new method has the potential to take advantage of DIC's strengths (low cost equipment and sample preparation) while eliminating its major weaknesses (limited 3D analysis). These benefits make this new method a powerful tool for studying prosthetic design.

3. Experimental and Computational Methods

Based on our literature review of existing technologies for structural analysis, we determined that the MultiDIC technology developed by Solav et al. [33] was a promising tool to calculate the factor of safety in prosthetic socket designs. However, since that paper did not address failure analysis, we needed to determine if the tool was capable of characterizing structural failures. A validation study (outlined in **Appendix A.1**) was conducted which demonstrated that MultiDIC was an effective tool for structural failure analysis. Subsequent experiments were conducted to understand how prosthetic sockets fail in compression. In the first stage, a socket loading fixture was simulated using ABAQUS CAE. This simulation represents how current simulation model parameters predict the stress and strain distribution of prosthetic sockets. This computational work was followed by an experiment where a 3D printed polylactic acid (PLA) socket was compressed in the socket loading fixture until failure. This event was captured with a synchronized camera array. This analysis was limited to a single prosthetic socket to determine the viability of the 360º 3D DIC method. The MultiDIC software used the camera data to reconstruct a 360º strain map of a prosthetic socket. Finally, the simulated data was compared to the experimental data to understand the current limitations of existing structural analysis methods.

3.1 Simulation

ABAQUS CAE requires objects to be represented by a parametric CAD file before it can simulate their mechanical behavior. To create a parametric CAD file of an amputee's limb, a geometry was generated using spline decomposition of a parent .STL file. This decomposition

method was used to generate parametric CAD files of all the socket loading fixture components. Once all of the geometries were created, the CAD files were imported into ABAQUS CAE for analysis (**Figure 2**).

Dickinson et al. [6] presented several references where researchers assumed that the material behavior was homogeneous and isotropic when simulating prosthetic sockets. Based on previous assumptions [6], the following simulations also utilize homogenous and isotropic material properties (**Table 1**). The interaction between the socket and residual limb was defined as surface to surface with finite sliding. The behavior of the contact surface simulation was set as tangential with zero tolerance for adjustment. Additionally, a zero frictional penalty was defined resulting in rigid and perfect contact between simulated surfaces.

Both models for the residual limb and socket had a tetrahedral mesh geometry and a global seed size of 0.0075. The model components had 40405 and 13649 elements respectively which was sufficient to enable convergence of simulated results. To avoid convergence errors mentioned in previous work [8], the number of iterative attempts was increased from the default of 5. A load of 2240 N was applied to the top surface of the residual limb model under the assumption that the aluminum rod used was able to transfer loads perfectly. This force value is the structural proof strength as specified by ISO 10328. Finally, the flat plane at the bottom of the distal end of the socket was specified as a fixed boundary condition.

3.2 Physical Experiment

A physical experiment was conducted to characterize the full surface strain of a 3D printed prosthetic socket in pure compression using MultiDIC. Using the camera system built by Solav et al. [33] as inspiration, a synchronized camera system capable of capturing image data in a 360º field of view was built. Two rings of LED lights ensure that samples are evenly illuminated. 16 Raspberry Pi 3 B+ and cameras were arranged radially on an adjustable mounting system (**Figure 3**). All of the Raspberry Pi computers are connected on a local network via a network switch. A separate Raspberry Pi computer with a real time clock (RTC) module set the global time for the system using Network Time Protocol (NTP). A host PC initiates a Python script over Secure Shell Protocol (SSH) for capturing images at 1640x1232 resolution and 1 frame per second (**Appendix A.2**). **Figure 4** shows the network configuration.

The same socket design was analyzed in both the simulations and physical experiment. A polylactic acid (PLA) test specimen utilizing 100% infill was manufactured by a Raise3d Pro 2 Plus FDM 3D printer. To prepare the socket for DIC analysis, the specimen's surface was coated with white spray paint to which a speckle pattern was applied. Finally, a pyramidal adapter was attached to the base of the socket to allow for mounting into the socket loading fixture.

This socket loading fixture, based on the Skoglund [21] design, uses two ball and socket joints to isolate the prosthetic socket specimen from bending moments when loaded in compression (**Figure 5**). The fixture applies a uniform load to the prosthetic socket through a replica of a patient's limb cast in epoxy. An instrumented load cell (Instron 3367) transfers the load to the epoxy limb via an aluminum rod fixed centrally in the limb. The separate components of the apparatus connect to each other using standard prosthetic pyramidal adapters.

During the experiment, an instrumented load cell first applied a preload of 5 N to the socket specimen, then compressed this specimen at a quasistatic velocity of 0.11mm/s to a maximum extension of 45mm. The synchronized camera array captured images of the deformation for the MultiDIC analysis. The socket exhibited a structural failure during this loading cycle.

4. Results and Discussion

The simulated and experimental strain maps were plotted using ABAQUS CAE and the MultiDIC MATLAB toolbox. When compared, these two strain maps showed similar strain profiles (**Figure 6**). This agreement suggests that the multibody simulation model is able to accurately impose a loading condition similar to the real-world experiment. However, comparing the numerical data between the two profiles, the simulated strain is significantly smaller than the observed experimental strain (**Figure 6**) The maximum simulated strain was $2.5*10^{-4}$ while the maximum experimental strain was $5.7*10^{-3}$, one order of magnitude higher. This difference implies that the homogeneous isotropic material properties assumed by many previous researchers are not sufficient to accurately characterize the structural behavior of prosthetic sockets. Thus, one way to improve simulated models is to determine the anisotropic material properties of printed specimens and incorporate this data into simulations. Following this result, the mechanical properties of the PLA specimens were measured using ASTM D638 [19] and found to have a lower Young's modulus and tensile strength than expected from the bulk material (**Table 2**).

Interestingly, the ultimate failure and delamination of the socket occurred at the bottom of the distal end, even though the simulated model and the experimental model show the highest surface strain concentration in a different location (**Figures 6 & 7**). This discrepancy means that the true strain concentration that led to failure occurred on the inside of the socket. **Figure 8** shows several small breaks before the large delamination event. These breaks could potentially be from the attachment screws destroying individual printed layers on the inside of the socket. The prosthetic socket specimen failed at 694.4 N which is lower than the 2240 N proof strength required by ISO 10328. Since the prosthetic socket failed at a low force under quasistatic loading conditions, it would not be capable of surviving the 1330 N cyclic loading requirement. Based on this observation, a new boundary condition for the distal end attachment should be utilized to identify interior stress concentrations. Clearly, there are both structural and material deficiencies that need to be addressed in 3D printed prosthetic sockets.

One limitation of the 360º 3D strain analysis is that the surfaces did not perfectly align during reconstruction (**Figure 9**). This could be due to the prosthetic socket being positioned off the central axis whereas the calibration object was positioned in the center of the camera array. The calibration object was slightly smaller than the prosthetic socket, but this should not have had any effect on calculating camera parameters because the calibration object was equally within the field of view of all cameras. It is important to note that while changing these factors can improve the quality of the visualization, the quantitative strain values will remain unchanged. Engineers can utilize this quantitative strain data to make design adjustments to improve the safety and mechanical performance of prosthetic sockets. Overall, 360° 3D DIC improves the testing phase of the prosthetic socket design cycle by precisely identifying

limitations in assumptions for simulated models and by generating full field quantitative strain maps to highlight local strain concentrations.

5. Conclusions and Future Work

5.1 Conclusions

This research offers several significant advances to the field of prosthetics. A synchronized 360° camera array was built to record deformations on the surface of a prosthetic socket under compressive loading. Using MultiDIC and this camera data, a full field 360° strain map was reconstructed on a prosthetic socket specimen. These experimental strain maps are useful because they pinpoint specific strain concentrations on a sample. However, their greatest strength comes from comparisons with simulated strain maps. The prosthetic socket specimen was simulated using homogeneous isotropic material properties. Comparisons between the simulated strain data and the experimental strain data indicate that these assumptions are not sufficient to calculate an accurate numerical strain value. This insight would not have been possible without this new strain characterization technology. In conclusion, 360° 3D DIC enables engineers to have a clearer view of how an entire mechanical system performs. This technology allows them to make a distinction between failures due to material properties and failures due to structural design. 360° 3D DIC is useful for the field of prosthetics research and will empower engineers to create stronger, lighter, and safer designs.

5.2 Future Work

One limitation of the work reported herein is that the experimental socket model only accounts for a quasistatic loading condition. This stands in contrast with the dynamic nature of the human gait cycle. In addition, the model only accounts for failures under compressive loading conditions and does not account for failures due to bending or fatigue. Future research is needed to test prosthetic sockets under dynamic loading conditions and long term fatigue conditions. Additionally, future simulations must incorporate anisotropic material properties. Significant computational resources will be needed to visualize the dynamic experimental and simulation results. In future studies, 360° 3D DIC will be a critical tool to create accurate simulations and achieve a greater understanding of these complex mechanical systems. Ultimately, this technology will guide prosthetic safety research by allowing engineers to find innovative materials and improve the quality of all prosthetic designs.

6. Acknowledgements

References

[1] Jin Y, Plott J, Chen R, Wensman J, Shih A. Additive Manufacturing of Custom Orthoses and Prostheses - A Review. Procedia CIRP 2015; 36:199–204. https://doi.org/10.1016/j.procir.2015.02.125.

[2] Standards for prosthetics and orthotics. Geneva: World Health Organization; 2017.

[3] Andregård E, Magnusson L. Experiences of attitudes in Sierra Leone from the perspective of people with poliomyelitis and amputations using orthotics and prosthetics. Disability and Rehabilitation 2017;39:2619–25. https://doi.org/10.1080/09638288.2016.1236409.

[4] Michalski MH, Ross JS. The Shape of Things to Come: 3D Printing in Medicine. JAMA 2014;312:2213. https://doi.org/10.1001/jama.2014.9542.

[5] ISO 10328: Prosthetics – Structural testing of lower-limb prostheses – Requirements and test methods. Switzerland: International Standards Organization; 2006.

[6] Dickinson AS, Steer JW, Worsley PR. Finite element analysis of the amputated lower limb: A systematic review and recommendations. Medical Engineering & Physics 2017;43:1–18. https://doi.org/10.1016/j.medengphy.2017.02.008.

[7] Jamaludin MS, Hanafusa A, Shinichirou Y, Agarie Y, Otsuka H, Ohnishi K. Analysis of Pressure Distribution in Transfemoral Prosthetic Socket for Prefabrication Evaluation via the Finite Element Method. Bioengineering 2019;6:98. https://doi.org/10.3390/bioengineering6040098.

[8] Cagle JC, Reinhall PG, Allyn KJ, McLean J, Hinrichs P, Hafner BJ, et al. A finite element model to assess transtibial prosthetic sockets with elastomeric liners. Med Biol Eng Comput 2018;56:1227–40. https://doi.org/10.1007/s11517-017-1758-z.

[9] Van L, Yamamoto S, Hanafusa A. Finite Element Analysis for Quantitative Evaluation of a Transfemoral Prosthesis Socket for Standing Posture. IJCA 2017;170:1–8. https://doi.org/10.5120/ijca2017914658.

[10] Sengeh DM, Herr H. A Variable-Impedance Prosthetic Socket for a Transtibial Amputee Designed from Magnetic Resonance Imaging Data: JPO Journal of Prosthetics and Orthotics 2013;25:129–37. https://doi.org/10.1097/JPO.0b013e31829be19c.

[11] Moerman KM, Holt CA, Evans SL, Simms CK. Digital image correlation and finite element modelling as a method to determine mechanical properties of human soft tissue in vivo. Journal of Biomechanics 2009;42:1150–3. https://doi.org/10.1016/j.jbiomech.2009.02.016.

[12] Colombo G, Bertetti M, Bonacini D, Magrassi G. Reverse engineering and rapid prototyping techniques to innovate prosthesis socket design. In: Corner BD, Li P, Tocheri M, editors., San Jose, CA: 2006, p. 60560P. https://doi.org/10.1117/12.644175.

[13] Ali I, Kumar R, Singh Y. Finite Element Modelling and Analysis of Trans-Tibial Prosthetic Socket Finite Element Modelling and Analysis of Trans-Tibial Prosthetic Socket. Global Journal of Researches in Engineering: A Mechanical and Mechanics Engineering 2014;14:42–50.

[14] Faustini MC, Neptune RR, Crawford RH, Rogers WE, Bosker G. An Experimental and Theoretical Framework for Manufacturing Prosthetic Sockets for Transtibial Amputees. IEEE Transactions on Neural Systems and Rehabilitation Engineering 2006;14:304–10. https://doi.org/10.1109/TNSRE.2006.881570.

[15] van Heesewijk A, Crocombe A, Cirovic S, Taylor M, Xu W. Evaluating the Effect of Changes in Bone Geometry on the Trans-femoral Socket-Residual Limb Interface Using Finite Element Analysis. In: Lhotska L, Sukupova L, Lacković I, Ibbott GS, editors. World Congress on Medical Physics and Biomedical Engineering 2018, vol. 68/2, Singapore: Springer Singapore; 2019, p. 587–91. https://doi.org/10.1007/978-981-10-9038-7_109.

[16] Surapureddy R, Stagon S, Schönning A, Kassab A. Predicting pressure distribution between transfemoral prosthetic socket and residual limb using finite element analysis. IJECB 2016;4:32. https://doi.org/10.1504/IJECB.2016.10002681.

[17] Current TA, Kogler GF, Earth DG. Static structural testing of trans-tibial composite sockets. Prosthet Orthot Int 1999;23:113–22. https://doi.org/10.3109/03093649909071622.

[18] Goh JCH, Lee PVS, Ng P. Structural integrity of polypropylene prosthetic sockets manufactured using the polymer deposition technique. Proc Inst Mech Eng H 2002;216:359–68. https://doi.org/10.1243/095441102321032157.

[19] D20 Committee. Test Method for Tensile Properties of Plastics. ASTM International; n.d.

[20] Gerschutz MJ, Haynes ML, Nixon D, Colvin JM. Strength evaluation of prosthetic check sockets, copolymer sockets, and definitive laminated sockets. JRRD 2012;49:405. https://doi.org/10.1682/JRRD.2011.05.0091.

[21] Skoglund P. Prosthetic socket in Titanium : An outer shell prosthetic socket for a lower-leg amputee manufactured in Ti6Al4V by Electron Beam Melting. Student thesis. 2015.

[22] Agilent Technologies. Practical Strain Gage Measurements 1999.

[23] Davenport P, Noroozi S, Sewell P, Zahedi S. Monitoring the suitability of the fit of a lower-limb prosthetic socket using an artificial neural network in commonly encountered walking conditions. WCCM 2017 - 1st World Congress on Condition Monitoring 2017 2017.

[24] South RV, Coker EG, Filon LNG. A Treatise on Photo-Elasticity. The Mathematical Gazette 1932;16:277. https://doi.org/10.2307/3605934.

[25] Phillips JW. Chapter 6: Photoelasticity. Experimental Stress Analysis, University of Illinois at Urbana-Champaign; 1998.

[26] Dally JW, Riley WF. Experimental stress analysis. 4th ed. Knoxville, Tenn: College House Enterprises; 2005.

[27] Chu TC, Ranson WF, Sutton MA. Applications of digital-image-correlation techniques to experimental mechanics. Experimental Mechanics 1985;25:232–44. https://doi.org/10.1007/BF02325092.

[28] McCormick N, Lord J. Digital Image Correlation. Materials Today 2010;13:52–4. https://doi.org/10.1016/S1369-7021(10)70235-2.

[29]Blaber J, Antoniou A. Ncorr Instruction Manual 2014.

[30] Wang Y, Lava P, Coppieters S, Houtte PV, Debruyne D. Application of a Multi-Camera Stereo DIC Set-up to Assess Strain Fields in an Erichsen Test: Methodology and Validation. Strain 2013;49:190–8. https://doi.org/10.1111/str.12027.

[31] Luo PF, Chao YJ, Sutton MA, Peters WH. Accurate measurement of three-dimensional deformations in deformable and rigid bodies using computer vision. Experimental Mechanics 1993;33:123–32. https://doi.org/10.1007/BF02322488.

[32] Solav D, Moerman KM, Jaeger AM, Herr HM. A Framework for Measuring the Time-Varying Shape and Full-Field Deformation of Residual Limbs Using 3-D Digital Image Correlation. IEEE Trans Biomed Eng 2019;66:2740–52. https://doi.org/10.1109/TBME.2019.2895283.

[33] Solav D, Moerman KM, Jaeger AM, Genovese K, Herr HM. MultiDIC: An Open-Source Toolbox for Multi-View 3D Digital Image Correlation. IEEE Access 2018;6:30520–35. https://doi.org/10.1109/ACCESS.2018.2843725.

[34] Boyer HE, Gall TL, American Society for Metals, editors. Metals handbook. Desk ed. Metals Park, Ohio: American Society for Metals; 1984.

[35] Raise3D Premium PLA Technical Data Sheet 2019.

[36] EpoxAcastTM 655 Metal Filled Castable Epoxy n.d.

[37] Chen Z, Gabbitas B, Hunt D. The fracture of wood under torsional loading. J Mater Sci 2006;41:7247–59. https://doi.org/10.1007/s10853-006-0913-y.

[38] Porter MM, Meraz L, Calderon A, Choi H, Chouhan A, Wang L, et al. Torsional properties of helix-reinforced composites fabricated by magnetic freeze casting. Composite Structures 2015;119:174–84. https://doi.org/10.1016/j.compstruct.2014.08.033.

Figure 1: Two lower limb (trans-tibial) prosthetics manufactured using traditional shaping methods. **a)** The socket on the left is made of a laminated carbon fiber composite which is expensive but common in developed nations. **b)** The socket on the right is manufactured at a low cost out of high density polyethylene (HDPE) by Jaipur Foot in India
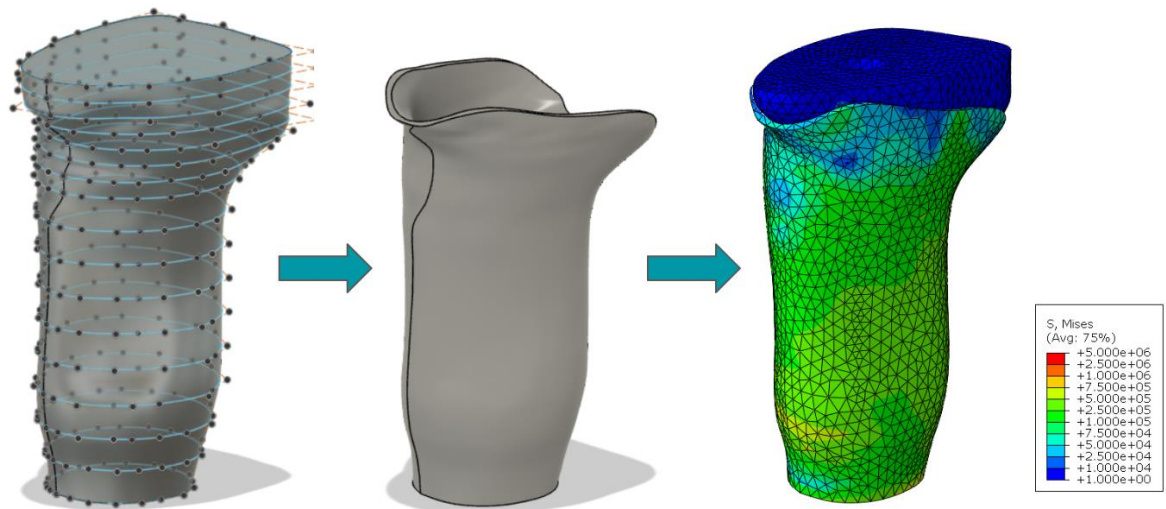
Figure 2: Example of residual limb geometry transformed into a parametric CAD using splines. This geometry was then meshed for the simulations in ABAQUS CAE.

**Table 1:** Table displaying material properties utilized in the simulations

| Material	Density (kg/m³)	Young's Modulus (GPa)	Poisson's Ratio
Aluminum (6061) [34]	2700	68.9	0.33
PLA [35]	1200	2.636	0.36
EpoxACast™ 655 [36]	1660	14.1	0.3* (Approx)
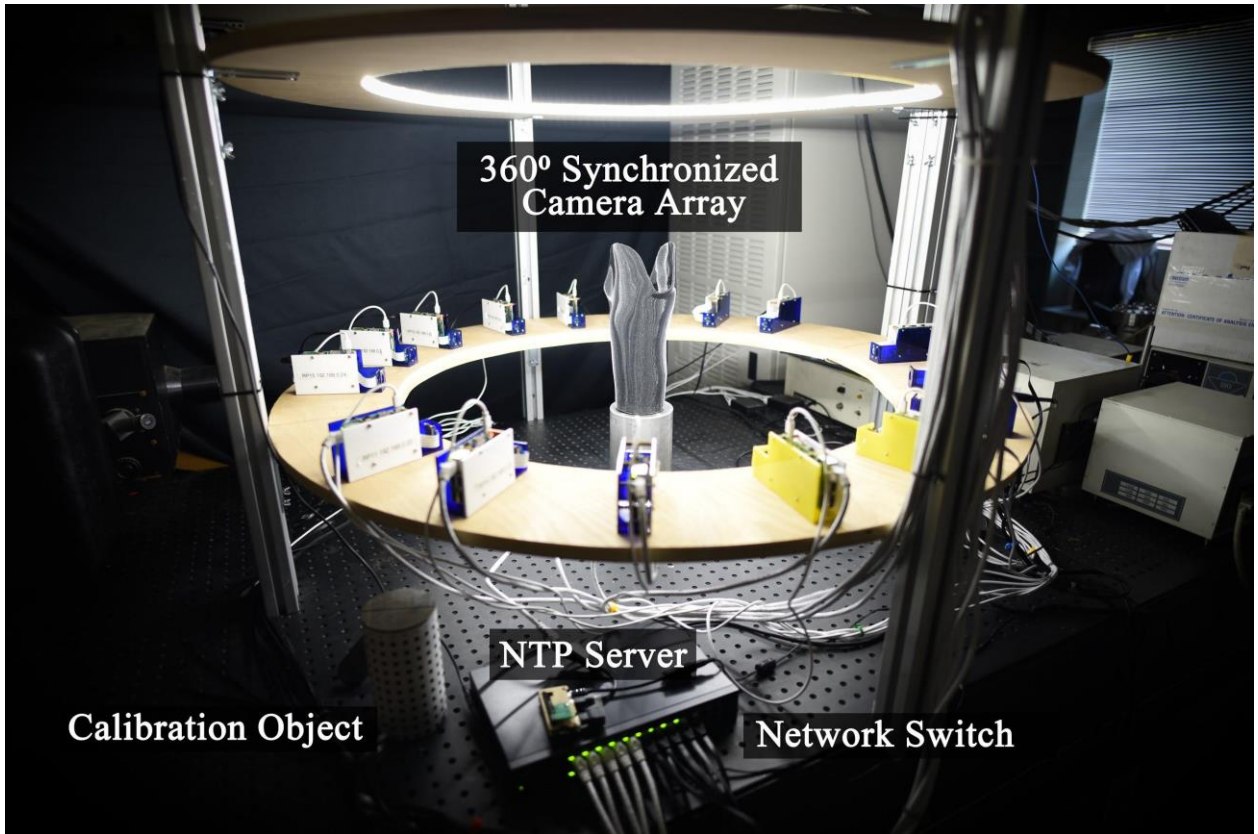
Figure 3: 360° Synchronized Camera Array. This camera system consists of 16 Raspberry Pi computers and PiCamera v2 modules connected in a local network. These computers are time synchronized via a Raspberry Pi acting as an NTP server.
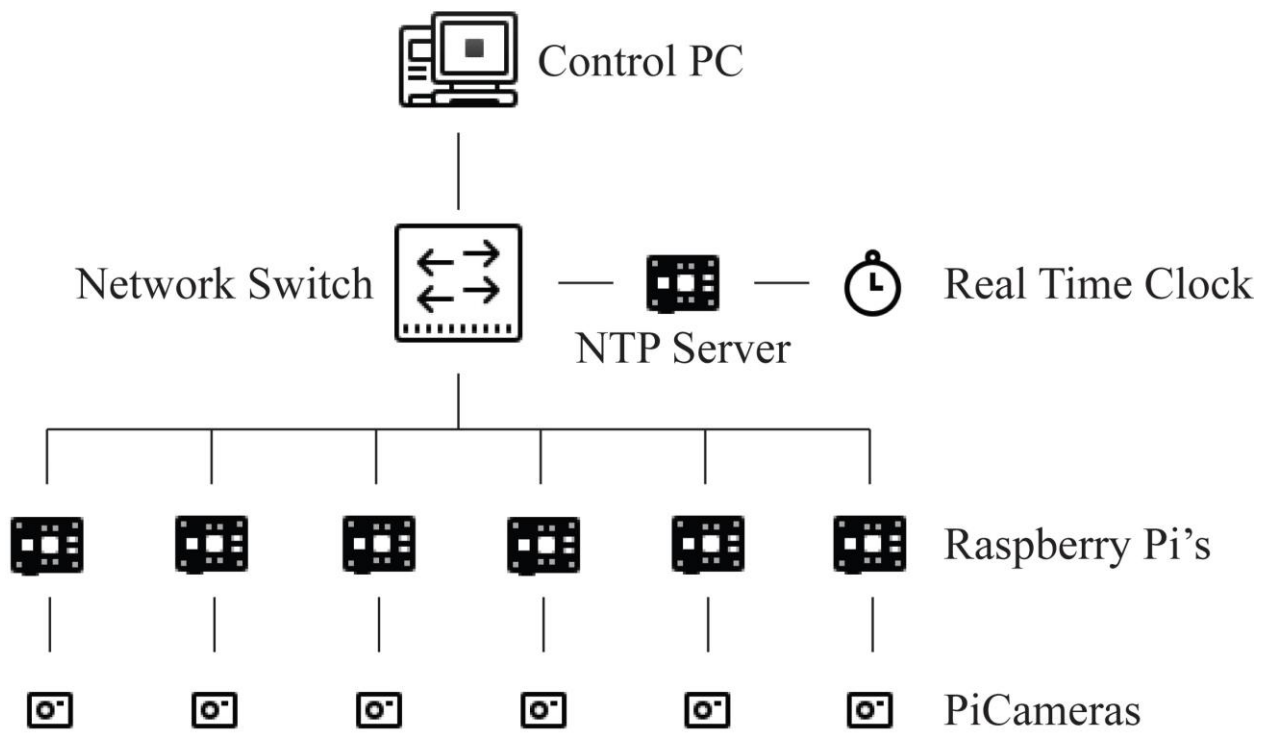
Figure 4. Network diagram showing the design of synchronized camera array. In this figure, the host PC interacts over SSH to control a network of Raspberry Pi computers and PiCameras, while the network is synchronized by the NTP server.
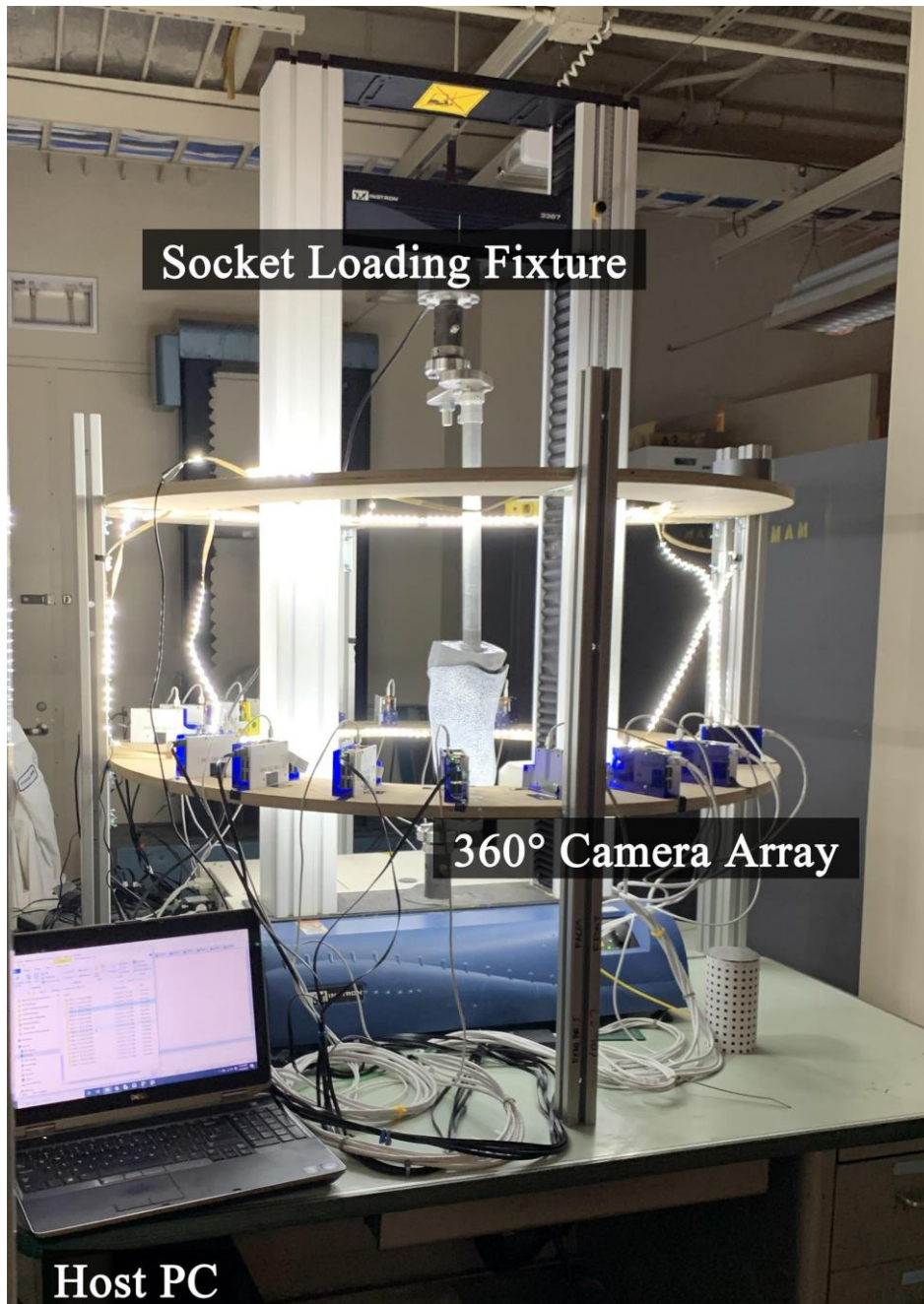
Figure 5: Image showing the experimental setup for testing prosthetic sockets in compression. This socket loading fixture is surrounded by our 360° synchronized camera array to facilitate 3D digital image correlation analysis.
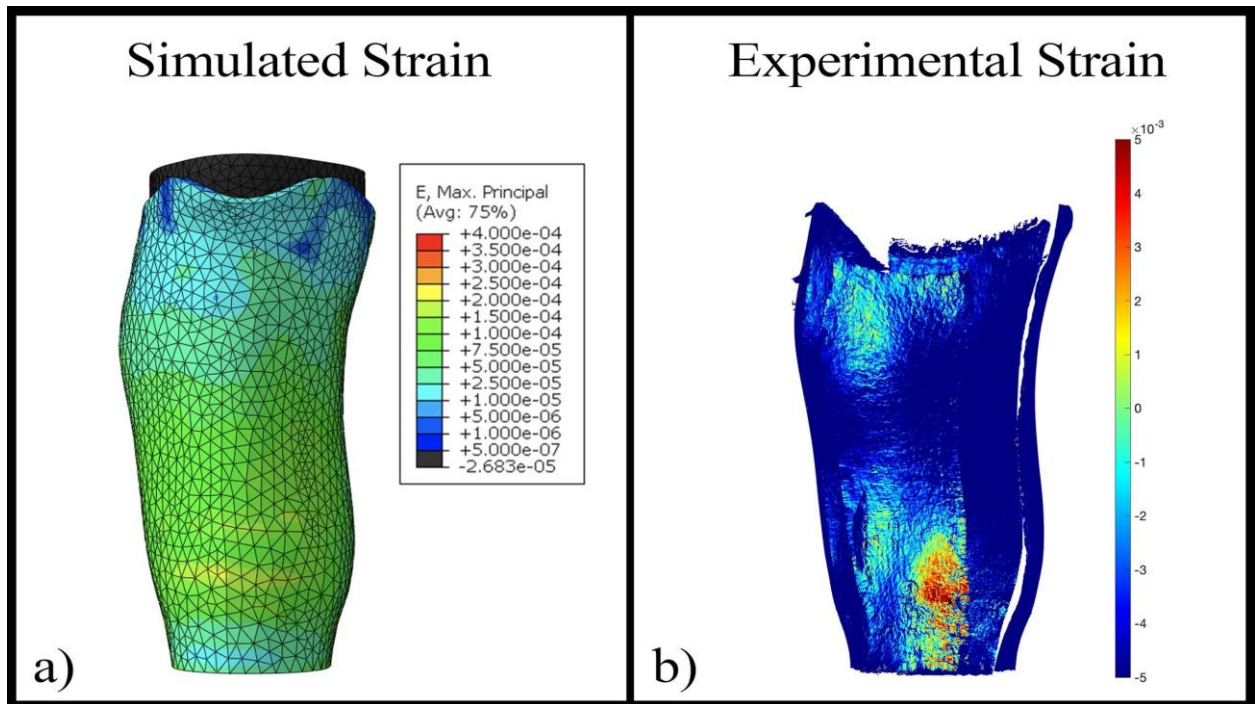
Figure 6: Image showing a comparison between experimentally generated strain maps and simulated strain maps. These two graphics show great agreement as to the strain distribution, but the simulated strain is much smaller than the experimental strain.

Table 2: Table showing the bulk material PLA properties versus properties of the printed materials. The prosthetic socket test specimen was printed in the horizontal orientation. These results were obtained using ASTM D638.

| Material Properties	Young's Modulus GPa	Tensile Strength MPa
Bulk from Literature [35]	2.64 ± 0.33	46.6 ± 1.2
Vertical Print Orientation	2.11 ± 0.11	47.5 ± 1.2
Horizontal Print Orientation	1.95 ± 0.06	22.1 ± 1.0
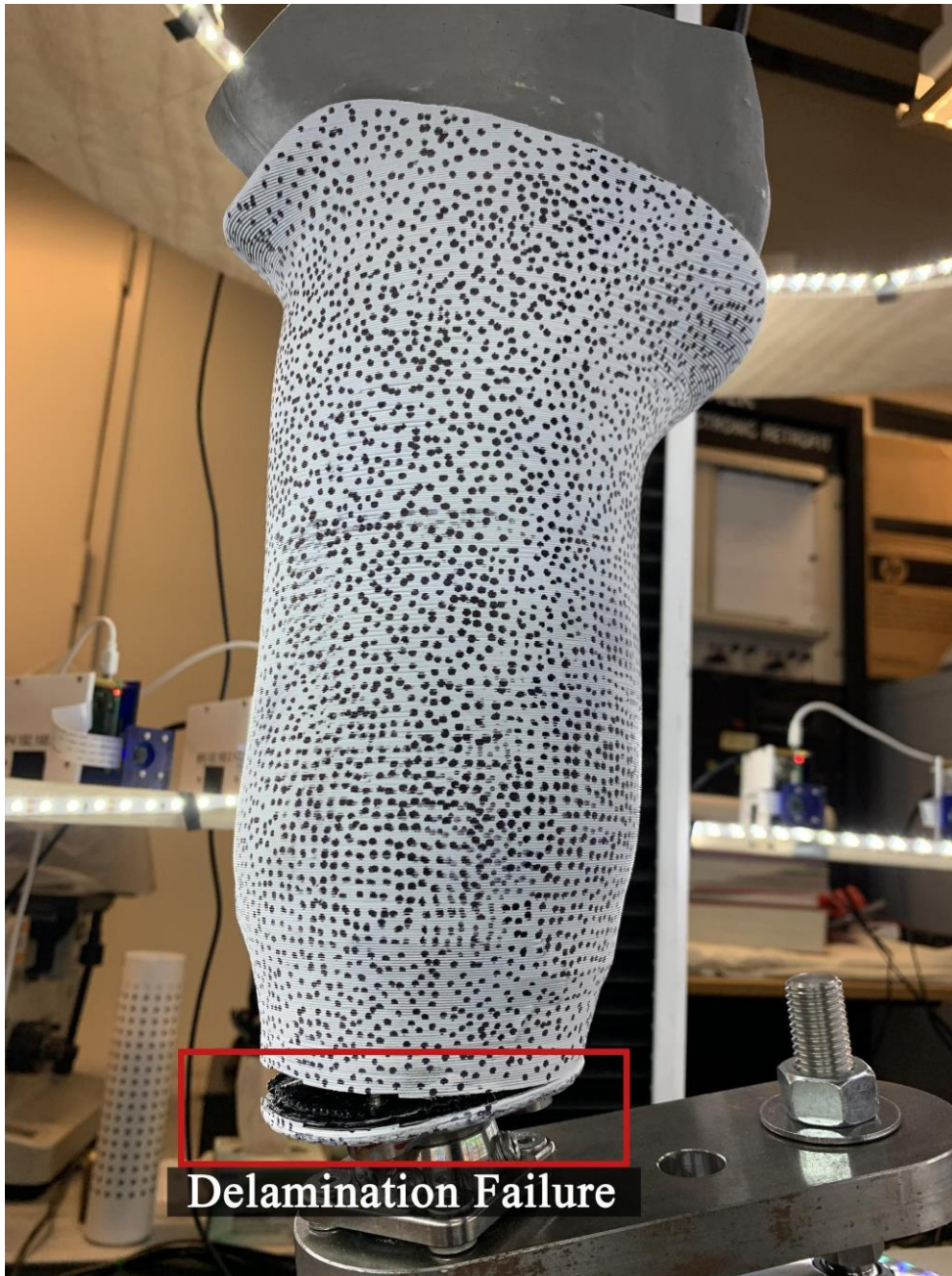
Figure 7: Image showing the delamination failure at the distal end of the tested prosthetic socket. Although both the simulation and the experiment observed high strain in a different region, the socket delaminated completely at the distal end indicating there was an internal stress concentration due to the attachment mechanism.
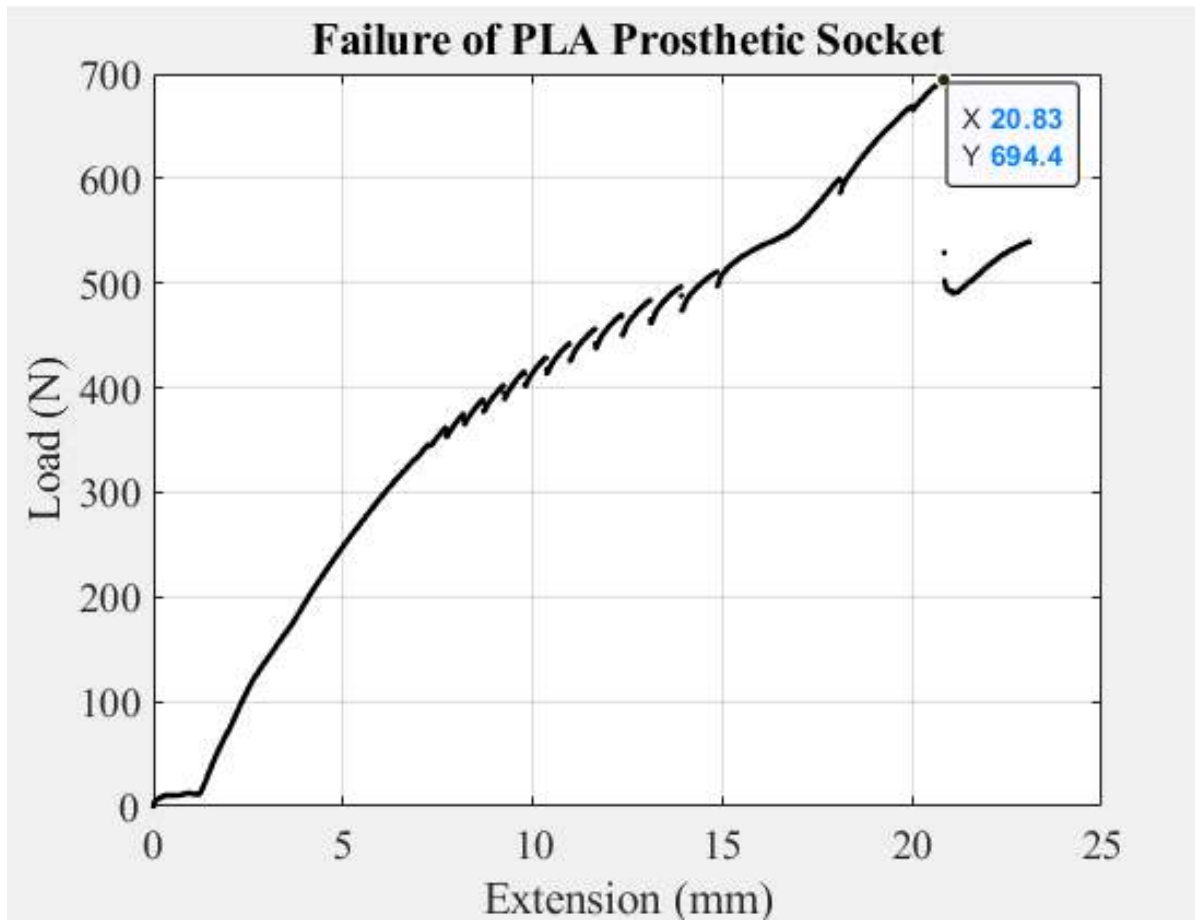
Figure 8: Graph displaying the load-displacement curve from the Instron. The prosthetic socket failed at 694.4 N which is much less than the 2240 N proof strength specified by ISO 10328.
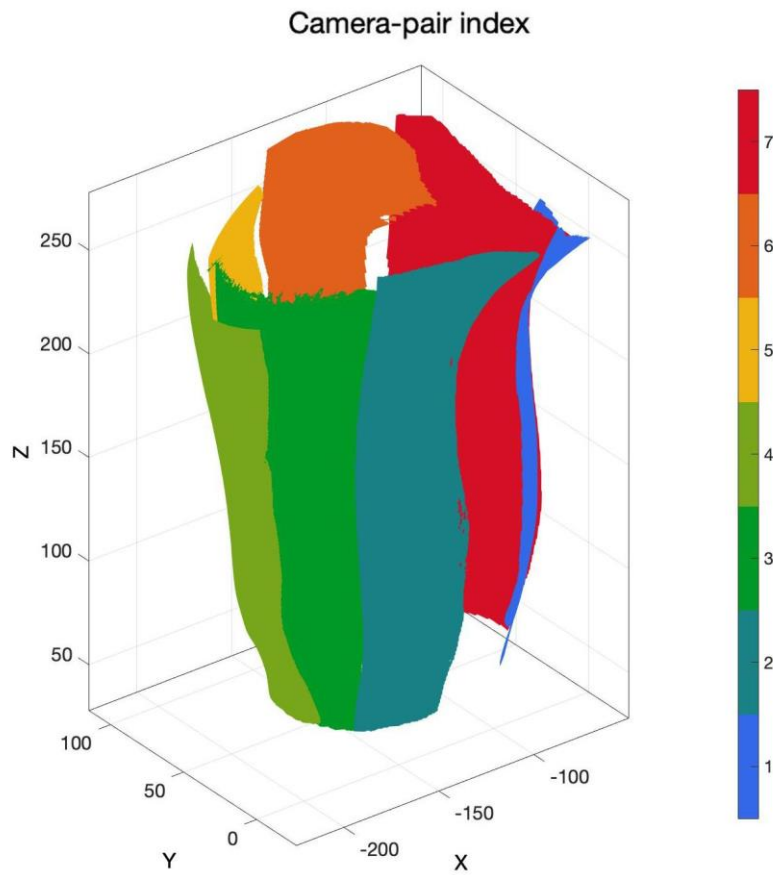
Figure 9: Image showing reconstructed 360° 3D geometry. While the surfaces do not perfectly align into the original shape, the numerical strain values are valid.

Appendix

A.1 Validation of MultiDIC Method for Failure Analysis

From our literature search, we found that there were many underutilized technologies that would be incredibly useful for characterizing the failure mechanisms of prosthetic sockets. Specifically, we determined that the MultiDIC technology developed by Solav et al. [33] would be the most groundbreaking for structural failure analysis of complex 3D objects. However, this paper did not include analysis of deformation and failure in an instrumented load cell. Because of this limitation, we needed to run our own validation study to determine whether MultiDIC could be utilized for structural failure analysis. In our validation study, we chose to characterize the torsional failure mode of balsa wood utilizing a 180° camera setup. This work was important because MultiDIC needed to be able to characterize known failure mechanisms in order to be used as a tool for critical safety analyses of prosthetics.

A.1.1 Design of 180⁰ Synchronized Camera Array

Drawing inspiration from Solav et al. [33] we built a synchronized compact 180° camera array designed to capture photos in a torsional testing configuration. This array is built on a semicircular frame that is designed to be adjustable to accommodate for different sample heights. On the frame, six Raspberry Pi 3 Model B+ computers, each equipped with camera module v2's, are equally spaced 30° apart. These Raspberry Pi's are routed together via a local network switch and time synchronized using another Raspberry Pi 3 Model B+ computer functioning as a Network Time Protocol (NTP) server. All Raspberry Pi machines are controlled remotely using a host PC communicating with the local network (**Figure 4**). This host PC controls a Python script that initiates the image capture program (See **Appendix A.2**). With this script, we capture synchronized images at 1640x1232 resolution and 1 frame per second. The main advantages of this system is that it is low cost (~$500 for 6 cameras) and is scalable (up to 48 cameras on a single switch.)

A.1.2 Testing Known Failure Mechanism: Torsion

Wood structures can fail reliably when loaded in torsion. Chen et al. [37] investigated the fracture of wood under torsional loading extensively and determined that cylindrical wood samples consistently generate longitudinal cracks when the wood grain is parallel to the twist axis. This meant that wood was an excellent candidate material to consistently generate longitudinal cracks.

To test the torsional configuration, the camera array needed to be calibrated for the specific camera geometry. We utilized a precision machined calibration object with known dimensions to determine the camera locations in relative space (**Figure A1**) In addition, we corrected for camera lens distortion as recommended by Solav et al. [33].

We prepared cylindrical balsa wood samples 70 mm in length, and 32 mm in diameter for torsional analysis and loaded it into a custom torsional load cell built by Porter et al. [38].

The sample was twisted at a rate of 0.002 radian/s and we ran our experiment until we reached 1 radian of extension. This was sufficient to consistently generate cracks.

### *A.1.3 Results and Implications for Prosthetic Research*

Once we finished the torsional experiment, we visualized the strain results using the MultiDIC toolbox developed by Solav et al. [33]. This required that we calculate lens distortion, calibrate our camera positions, calculate the 2D DIC maps for each stereo camera pair, reconstruct our 3D surface geometry, before we could project these strain maps onto the 3D surface. We evaluated the torsional specimen from its zero deformation state until right before failure. We were able to successfully visualize the results on an entire 180° surface; these are presented in **Figure A2.**

In **Figure A2,** we can clearly see that a crack propagated longitudinally across the sample. This behavior was entirely expected based off of the work by Chen et al. [37]. Looking at the principal strain map, we can observe that the MultiDIC system was able to keep track of the surface strain over the entire testing period. The system is able to show the strain concentration leading to the crack. This means that we were able to successfully observe strain concentrations in the sample even before they presented themselves as macroscopic cracks.

Overall, this validation was a success and we were able to visualize the strain field on the surface of an object in torsion utilizing multiple stereo camera pairs. This allowed us to capture the failure mechanism in our torsionally loaded balsa wood samples. Our system is extremely useful in observing strain concentrations on complex structures and can show us exactly where a structure will fail. This in turn tells us where a structure can be redesigned to increase safety. Since we were able to successfully characterize a structural failure mechanism using an instrumented load cell and the MultiDIC toolbox, we were confident to continue our work and begin to characterize the failure mechanisms of a prosthetic socket.

Figure A1: Image showing the assembled 180° synchronized camera array with a precision machined calibration object. This camera array is designed to analyze torsional failure modes in materials.
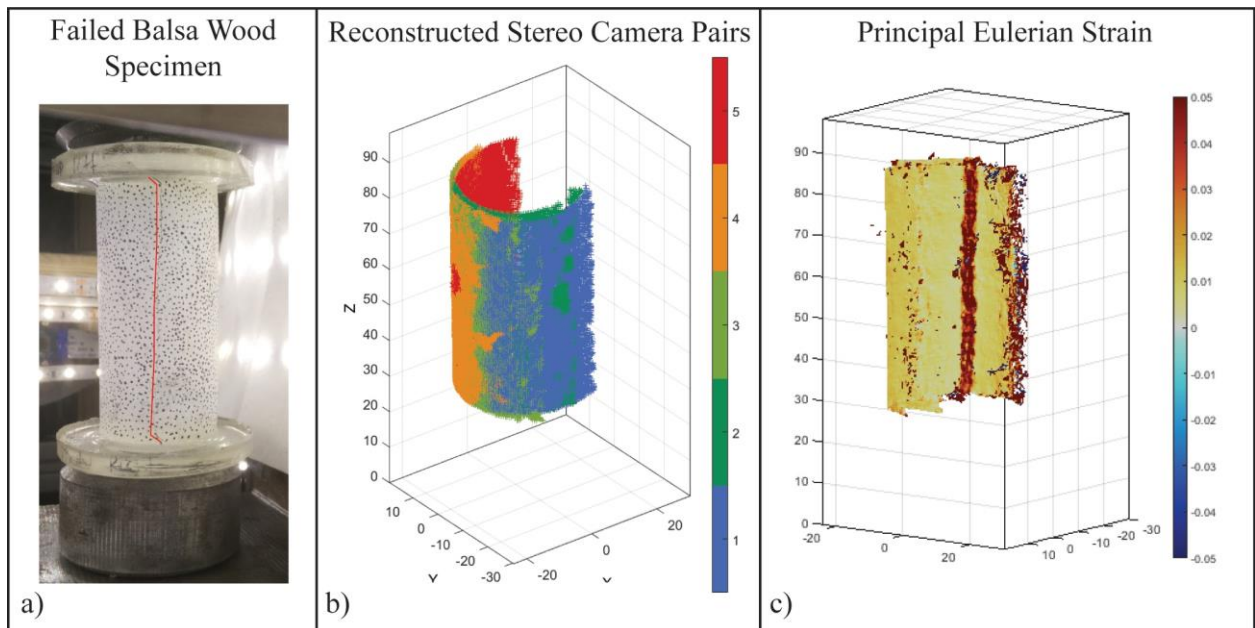
Figure A2: Image showing the (a) failed torsional specimen, (b) reconstructed 3D geometry, (c) successfully reconstructed 180° 3D strain map.

A.2 Python Image Capturing Program

Environment: Python 2.7

```python
import time
import numpy as np
import os
from datetime import datetime, timedelta
from picamera import PiCamera
from time import sleep
import socket
import math

# INSTRUCTIONS

#     THIS CODE INTENDED TO BE USED THROUGH SECURECRT
#     WHEN SENDING COMMANDS THROUGH TERMINAL TO ALL SESSIONS:
#         NEED TO MAP A KEY TO EMULATE KEYBOARD INTERRUPT IN SESSION
OPTIONS IN ORDER TO END CAPTURE SIMULTANEOUSLY
#         BASICALLY JUST TEDIOUS OTHERWISE GOING INTO EVERY COMMAND
LINE AND HITTING CRL+C
#         ON MAC THIS CAN BE DONE USING CRL+SHIFT+C MAPPING TO "\007"
#         YOU'LL NEED TO DO THIS FOR EVERY SESSION/PI
#         AFTER DOING THIS FOR EVERY SESSION HITTING THAT COMBINATION
WILL WRITE WHAT LOOKS LIKE A SPACE
#         HIT ENTER AND THE CAPTURE SHOULD END ON ALL OF THEM


camera = PiCamera()

#GETTING USER INPUT FOR RESOLUTION: 1 FOR FULL RES, 2 FOR HALF RES.

print "\nPlease enter resolution selection and hit enter: "
res = raw_input("Full resolution: 1. Half res: 2 \n")
try:
    res = int(float(res))
except:
    res = 3
restag = " "
if res == int(1):
    camera.resolution = (3280, 2464)
    restag = "Full"
    print "Capturing at Full resolution."
elif res == int(2):
```

```
        camera.resolution = (1640, 1232)
        restag = "Half"
        print "Capturing at Half resolution."
else:
        print "invalid, defaulting to Half resolution"
        camera.resolution = (1640, 1232)
        restag = "Half"


#GETTING SECONDS PER FRAME
spf = 1


#       print "\n[NOTE: SPF > 5 is more stable. Minimum SPF of 1 (default)]"
#       spf = raw_input("Enter the capture delay (seconds per frame), ex: 5 = 0.2fps: \n")
#       try:
#               spf = int(round(float(spf)))
#       except:
#               print "That is not a number but let's do this anyway"
#               spf = 1
#       if spf < 1:
#               spf = 1
#       elif spf > 60:
#               print "Are you sure you want over a 1 minute delay between captures?"
#               sure = raw_input("Type ""y"" if yes, anything else for no:")
#               if sure == "y":
#                       print "Well ok then..."
#               else:
#                       print "That's what I thought"


#       print "Your SPF is: " + str(spf)


#       CREATE DIRECTORY NAME
today = datetime.today()
todaystr = today.isoformat ()
todaystr = todaystr[0:16]

todaylist = list(todaystr)
todaylist[10] = '_'
todaylist[13] = '_'
todaystr = "".join(todaylist)


pi_label = socket.gethostname()


path = "/home/pi/Desktop/" + todaystr + "_" + pi_label + "/"
```

```python
#    CREATE DIRECTORY
try:
    original_umask = os.umask(0)
    os.makedirs(path, 0777)
except OSError:
    print ("Creation of the directory %s failed" % path)
else:
    print ("Successfully created the directory %s" % path)
finally:
    os.umask(original_umask)


#    CREATE INFO TEXT DOCUMENT
error_record = open(path + todaystr + "_" + pi_label + "_" + "experiment_info.txt","w+")

error_record.write(todaystr + pi_label +"\n")
error_record.write("Resolution: " + restag + "\n")
error_record.write("Seconds per Frame: " + str(spf) + "\n")


#    loop timing data analysis
testtime = []
tt1 = 0
tt2 = 0


#    setting variables keeping time for sleeping, naming, and errors

precapturetime = 0
postcapturetime = 0
post_errorcapturetime = 0
post_errortime = 0

timeforsleep = 0
ctime = 0 #capture time
errorctime = 0 #error capture time
capturetime = [] #list of capture times
#post_error_naming_adjust = 0 #name is self explanatory
#secondcapture = 0 #will be post_errorcapturetime - postcapturetime


print "Starting capture in:"  #This is here because we need to sleep >2 seconds to let camera
warm up
print "3..."
sleep(1)
print "2..."
sleep(1)
print "1..."
```

```python
sleep(1)
print "Starting Capture."

#MAIN CAPTURING LOOP, BREAK WITH CTRL + C (MUST CREATE KEY MAPPING
IN EACH SESSION IN SECURE CRT WITH CTRL + SHIFT + C ON MAC TO END
PROGRAM FROM COMMAND WINDOW)
try:
    tt1 = time.time()
    i = 1
    while True:

        precapturetime = time.time()
        camera.capture("%simage_%04d.jpg" % (path,i))
        postcapturetime = time.time()

        ctime = postcapturetime-precapturetime
        timeforsleep = float(spf) - (ctime)
        capturetime.append(ctime)

        if timeforsleep < 0:

            error_record.write("took " + str(timeforsleep) + " sec over " + str(spf) + " second
to capture image at frame: " + str(i) +"\n")
            print "..."

            post_errortime = time.time

            errorctime = post_errortime-precapturetime
            timeforsleep = math.ceil(errorctime) - errorctime

            sleep (timeforsleep)

            i = i + int(math.ceil(errorctime)) # spf must be 1, use modulus with spf to get
back to proper synchronous with SPF adjustments

            #secondcapture = post_errorcapturetime - postcapturetime

            #post_error_naming_adjust = int(math.ceil(errorctime))

            #camera.capture("%simage_%04d.jpg"                %                (path,i)
#+post_error_naming_adjust

            #post_errorcapturetime = time.time()
```

```python
            #capturetime.append(post_errorcapturetime-posterrortime) #log capture time
directly after error capture time


            #i = i + int(math.ceil(errorctime)) #- spf

            #if secondcapture > spf:
            #       error_record.write("took " + str(secondcapture) + " sec over " + str(spf) +
" second to capture image at frame: " + str(i) +"\n")

        else:
            i = i + spf
            sleep(timeforsleep)

        tt2 = tt1
        tt1 = time.time()
        testtime.append(tt1-tt2)

except KeyboardInterrupt:
    pass

error_record.write("average loop time: " +str(np.average(testtime)) + "\n")
error_record.write("stdev loop time: " + str(np.std(testtime)) + "\n")
error_record.write("average capture time: " + str(np.average(capturetime)) + "\n")
error_record.write("stdev capture time: " + str(np.std(capturetime)) + "\n")

error_record.write("capture times: \n")

for x in capturetime:
    error_record.write(str(x)+"\n")

camera.close()
error_record.close()
```

Declaration of interests

☒ The authors declare that they have no known competing financial interests or personal relationships that could have appeared to influence the work reported in this paper.

☐The authors declare the following financial interests/personal relationships which may be considered as potential competing interests: